Science Bulletin 70 (2025) 1410–1415

Contents lists available at ScienceDirect

Science Bulletin

journal homepage: www.elsevier.com/locate/scib

Science Bulletin
www.scibull.com

Short Communication

Highly tough and responsible ionic liquid/polyvinyl alcohol-based hydrogels for stretchable electronics

Pengcheng Zhou [a,b], Fan Mo [c], Zichong Ji [a,b], Jiawei Yang [a,b], Hongzhong Du [a], Zonglei Wang [a,b], Hossam Haick [b], Yan Wang [a,b,d,e,*]

[a] Department of Chemical Engineering, Guangdong Technion-Israel Institute of Technology, Shantou 515063, China
[b] The Wolfson Department of Chemical Engineering, Technion-Israel Institute of Technology, Haifa, 3200003, Israel
[c] Department of Biotechnology and Food Engineering, Guangdong Technion-Israel Institute of Technology, Shantou 515063, China
[d] Key Laboratory of Science and Engineering for Health and Medicine of Guangdong Higher Education Institutes, Guangdong Technion-Israel Institute of Technology, Shantou 515063, China
[e] Guangdong Provincial Key Laboratory of Materials and Technologies for Energy Conversion, Guangdong Technion-Israel Institute of Technology, Shantou 515063, China

ARTICLE INFO

Article history:
Received 13 November 2024
Received in revised form 14 December 2024
Accepted 17 January 2025
Available online 31 January 2025

Soft electronics have seen extensive development due to their lightness, outstanding mechanical flexibility, and biocompatibility, which make them ideal for a variety of applications, including health monitoring, human–machine interfaces, and advanced augmented reality/virtual reality communications [1,2]. Ionic liquid (IL)-based conductive hydrogels are typically made up of a polymer network swollen with IL, which are organic salts in a liquid state at or near room temperature, rather than traditional inorganic/organic salt electrolyte solutions [3–5]. These hydrogels leverage the unique properties of IL, such as high ionic conductivity, nonvolatility, and thermal stability, to create a flexible conductive material suitable for various applications in soft electronics, such as actuators, wearable sensors, and stretchable energy generation/storage devices [6–8].

To ensure device performance under repetitive mechanical deformations, it is essential to fabricate IL-based hydrogels with high mechanical properties and conductivity. IL-based hydrogels with stretchability exceeding 500% strain can be fabricated by self-catalytic cross-linking, double physical cross-linking, photopolymerization, and cyclic freeze–thaw strategies [9]. Moreover, recent efforts to enhance the toughness of these hydrogels have introduced strategies such as wet annealing, double-network structures, supramolecular interactions, and multiscale designs. Among them, cyclic freeze–thaw is a well-established physical cross-linking method that induces phase separation between polymer chains and solvents to improve the mechanical properties of hydrogels [10,11]. Wet annealing differs from traditional dry annealing as it promotes the rearrangement of the molecular or crystal structures within the material in a liquid environment. It is believed to provide freer movement of macromolecules for reorganization into stronger polymer networks [12]. Since no other conductive fillers are involved, the conductivity of IL-based hydrogels is determined by the physicochemical properties of the IL [3,13,14]. However, achieving IL-based hydrogels that simultaneously exhibit high stretchability, toughness, and conductivity remains some challenges that need to be addressed, as concluded in Table S1 (online). This challenge lies in balancing these critical properties with existing materials and manufacturing techniques.

The safety of IL-based conductive hydrogels is also a critical consideration for soft electronics, especially in wearable applications. As the field of soft electronics advances, developing responsible IL-based hydrogels that are both biofriendly and recyclable remains a top priority. Considering the toxicity of certain commonly employed ILs, the selection of suitable ILs is crucial in the fabrication of biocompatible ionic soft electronics [6]. In addition, recycling IL-based hydrogels after device service life is an effective strategy to reduce electronic waste (e-waste) and realize environmental sustainability. A 1-hexyl-3-methylimidazolium bromide-based hydrogel was prepared via a one-pot method, achieving a stretchability of over 500%. The waste hydrogel was dissolved and concentrated through hot water mediation, and the mechanical properties of the recycled IL-based hydrogel showed no significant reduction [10]. Nevertheless, IL-based hydrogels that combine optimal biocompatibility, recyclability, conductivity, and mechanical performance remain scarce in the existing literature.

---

* Corresponding author.
E-mail address: wang.yan@technion.ac.il (Y. Wang).

https://doi.org/10.1016/j.scib.2025.01.058

Therefore, it is still of great significance to produce IL-based hydrogels that achieve the aforementioned all-encompassing properties.

Polyvinyl alcohol (PVA) is increasingly recognized as a promising material for applications in gel-based soft electronics due to its unique properties in biocompatibility, non-toxicity, cost-effectiveness, and hydrophilicity [2,15]. Tough PVA gels can be fabricated by salting out [16], solvent-exchange [12], etc., but often involve time-consuming gelation or replacement processes. Herein, we report a facile strategy to obtain highly tough and responsible hydrogels by physically cross-linking IL, i.e., 1-butyl-3-methylimidazolium tetrafluoroborate ($BMIMBF_4$), with PVA, followed by wet annealing and cyclic freeze-thaw strategies. The obtained IL/PVA hydrogels, leveraging the unique combination of properties of $BMIMBF_4$ and PVA, exhibit excellent tensile strength of 4.99 MPa, high toughness of 2.52 MJ m^{-3}, stretchability of up to 1100% strain, negligible hysteresis, and high conductivity (31.85 mS cm^{-1}), as well as exhibiting excellent antimicrobial properties, strain sensing capabilities, and the ability to build all-in-one supercapacitors. This research is expected to inspire the design of cutting-edge wearable or implantable electronic devices that are comfortable, safe, and environmentally friendly.

$BMIMBF_4$/PVA hydrogels were strengthened synergistically through wet annealing and freeze–thaw strategies. As illustrated in Fig. 1a, PVA was first dissolved in deionized water to form a homogeneous solution with a mass fraction of 10%, creating extended macromolecular chain conformations and preassembled interlaced networks while eliminating noncovalent interactions within and between polymers (Fig. 1a(i) and Fig. S1a online). Subsequently, equal volumes of PVA solution and $BMIMBF_4$ aqueous solution (with varying concentrations) were gradually mixed, resulting in a viscous sol by removing the supernatant water layer (Movie S1 online). The physical cross-linking of PVA with hydrophilic IL ensured the formation of an interconnected polymer network (Fig. 1a(ii) and Fig. S1b online).

The concentration of IL heavily influences the occurrence of gelation. Gelation could not occur at a $BMIMBF_4$ concentration of 30%. Four $BMIMBF_4$ concentrations (40%, 50%, 60%, and 70%) caused gelation, and gelation was faster as the IL ratio increased (Fig. S2a online). This is due to the fact that water is a good solvent for PVA, while $BMIMBF_4$ is a poor one. At 30% IL, the high degree of solvation prevents gelation, resulting in a lower viscosity mixture than aqueous PVA solution. As the IL content increases, the degree of solvation of the mixture gradually decreases, triggering the formation of a gel. However, too much IL (60% and 70%) leads to insufficient exposure of functional groups, resulting in extremely viscous or even rigid gels (Fig. S2b online). Therefore, a 50 vol% $BMIMBF_4$ solution and a 10 wt% PVA solution were selected in equal volumes to prepare the target IL/PVA hydrogel for further study.

The cross-linking mechanism is driven by the cations of the ionic liquid ($[BMIM]^+$), which can form hydrogen bonds with the hydroxyl groups on PVA, resulting in strong interactions between PVA chains. Furthermore, this interaction reduces the solubility of PVA in solution, causing it to precipitate and form a hydrogel. The resulting viscous sol further underwent wet annealing to achieve structural densification by adjusting the macromolecular conformation (Fig. 1a(iii) and Fig. S1c online). Finally, through a cyclic freeze–thaw strategy, the weak semifluid gel was transformed into an ultra-strong and tough gel with high chain entanglement and highly crystallized PVA segments (Fig. 1a(iv) and Fig. S1d online).

For ease of description and discussion, pure PVA hydrogel and IL/PVA hydrogels obtained through freeze–thaw cycle without wet annealing process were denoted as PHF_x, and PIF_x, respectively. IL/PVA hydrogels obtained through the synergistic effect of wet annealing and freeze–thaw cycles were named $PIWF_x$. x represented the number of freeze–thaw cycles. Further solvent exchange of $PIWF_3$ hydrogel by replacing the water phase with $BMIMBF_4$ was also investigated. Although the resulting IL/PVA ionogel showed higher tensile strength, it exhibited a significant loss in elasticity and toughness (Fig. S2c online). Based on the reversible physical cross-linking network of $BMIMBF_4$/PVA hydrogel, it can be easily switched between solid and liquid states through heating and freezing processes, as shown in Fig. 1b, demonstrating its excellent processability and recyclability. This strategy may provide a promising approach to construct green, recyclable electronics to solve the problem of e-waste contamination.

The $PIWF_3$ hydrogel can be bent, knotted, twisted, and can withstand stretching over 10 times its original length (Fig. S3 online). Meanwhile, it could support a large bottle of water (total weight of 2.5 kg) over 800-fold its own weight (Fig. 1c), intuitively demonstrating the excellent mechanical properties of the obtained IL/PVA hydrogel. Fig. 1d shows the typical stress–strain curves of $PIWF_x$ hydrogels, and the results are summarized in Table S2 (online). $PIWF_1$ hydrogel possessed a tensile strength of 3.62 MPa and a fracture strain of 876%, respectively. The tensile strength and fracture strain are 3.88 times and 3.26 times those of PHF_1 hydrogel, respectively, indicating that the physical cross-linking between PVA and IL introduced numerous entanglement sites. On the other hand, as the number of freeze–thaw cycles increases, the toughness of IL/PVA hydrogels increases significantly. The tensile strength of $PIWF_5$ hydrogel is as high as 5.46 MPa, which is more than 1.51 times that of $PIWF_1$ hydrogel. This can be attributed to the microphase separation of IL/PVA hydrogels induced by cyclic freezing and thawing, making chains more tightly entangled. In addition, the fracture strain of IL/PVA hydrogels showed a trend of first increasing and then decreasing with the number of freeze–thaw cycles, reaching the maximum value of 1100% for $PIWF_3$ hydrogel. The elastic modulus and toughness of $PIWF_3$ hydrogel are significantly improved compared to PIF_3 and $PIWF_1$ hydrogels, reaching 2.83 MPa and 2.52 MJ m^{-3}, respectively (Fig. 1e). For the recycled IL/PVA hydrogel, its tensile properties, including strength and strain, were slightly reduced compared to the original hydrogel (Fig. 1d, e). Nevertheless, both the original hydrogels and the recycled IL/PVA hydrogels are competitive with the recent representative organic/inorganic filler ion-conducting PVA hydrogels (Fig. 1f). [2,8,9,15,17]. In addition, the performance of IL/PVA hydrogels after multiple recycling was verified through repetitive-fabrication-cycle, and it was found that they have similar mechanical properties (Table S3 online). This is because during the recycling process, the failed hydrogel structure will be rebuilt, thus achieving the goal of recycling use and reducing the impact on the environment. It is evident that IL/PVA hydrogel synthesized in this study is quite competitive in terms of mechanical strength, which makes it well-suited under extreme mechanical deformations.

The energy dissipation mechanism of $PIWF_3$ hydrogel was studied using a loading–unloading tensile test. In the stretching range from 10%–50% strain, $PIWF_3$ hydrogel showed small hysteresis loops, indicating that the high-density network provides effective energy dissipation (Fig. S4a online). To evaluate the fatigue resistance of $PIWF_3$ hydrogel, it was subjected to 50 consecutive tensile cycles (Fig. S4b online). The results showed that, except for the first loading–unloading cycle, the subsequent cycles showed minimal deviation, indicating consistent mechanical behavior. The results evidence that $PIWF_3$ hydrogel exhibited excellent fatigue resistance through reversible non-covalent interactions. Fig. S4c (online) shows the corresponding energy dissipation calculated based on the loading–unloading curve of $PIWF_3$ hydrogel. Surprisingly, $PIWF_3$ hydrogel exhibits low energy dissipation of 624.52 J m^{-2}. This is primarily due to the breaking of sacrificial

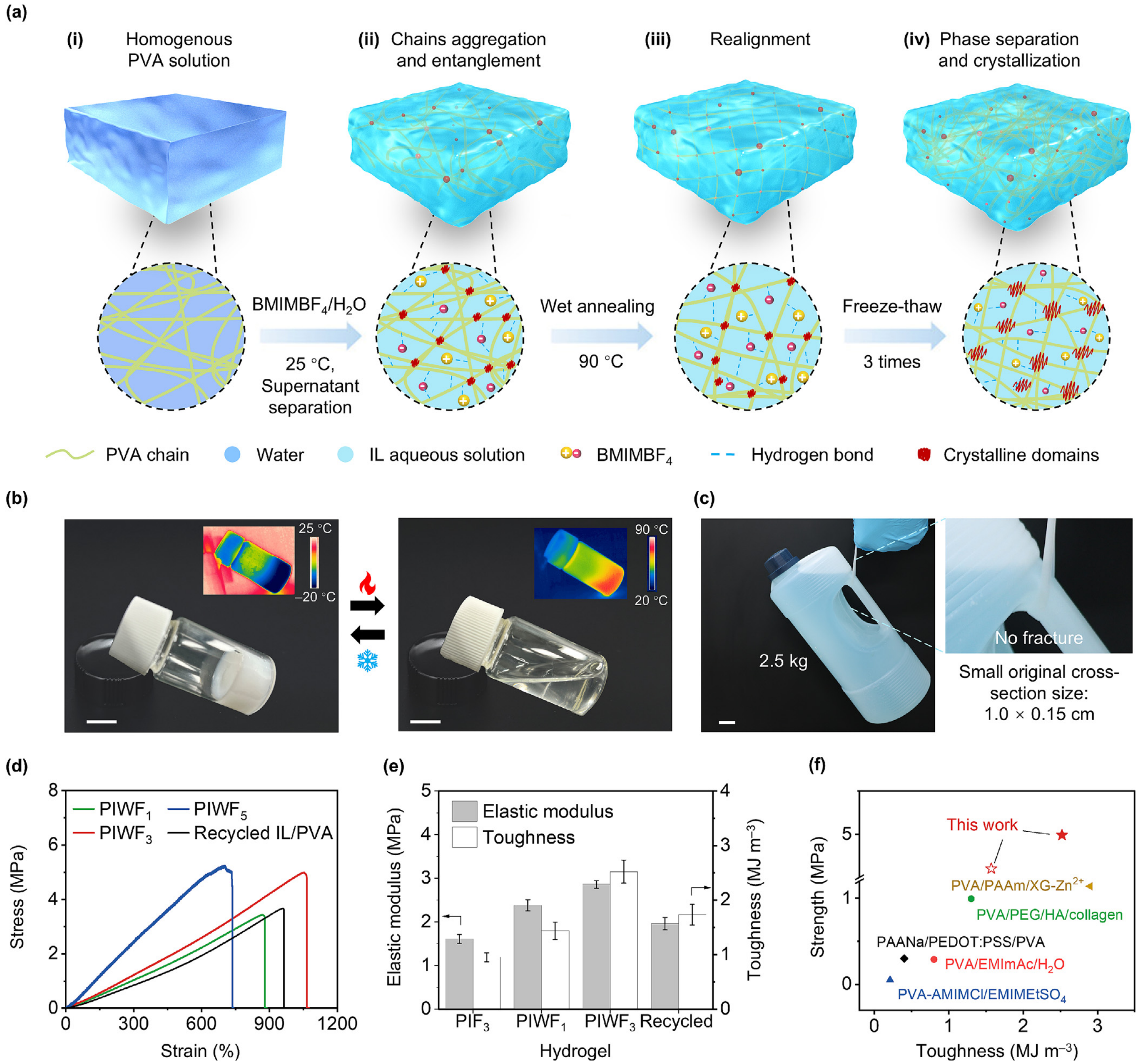

Fig. 1. Fabrication and mechanical properties of IL/PVA hydrogels. (a) Schematic diagram of the freeze–thaw assisted wet annealing synthesis strategy for tough, recyclable and bio-friendly IL/PVA hydrogels. (i) PVA/H$_2$O homogeneous solution with disordered pre-dispersed network. (ii) Crosslinking of PVA with BMIMBF$_4$ to form IL/PVA hydrogels precursor. (iii) Wet annealing to adjust macromolecular conformation in precursors. (iv) IL/PVA hydrogels with high macromolecular entanglement and crystallinity obtained by cyclic freeze–thaw strategy (PVA: polyvinyl alcohol; BMIMBF$_4$: 1-butyl-3-methylimidazolium tetrafluoroborate). Photographs show the state of the hydrogels during their formation. (b) Photograph of PIWF$_3$ hydrogel under heating and freezing states. Scale bar: 1 cm. (c) Photographs demonstrating the mechanical robustness of IL/PVA hydrogels and their ability to suspend 2.5 kg of water. Scale bar: 1 cm. (d) Tensile stress–strain curves of PHF$_1$, PIWF$_x$ and recycled IL/PVA hydrogels. (e) Elastic modulus and toughness of PHF$_1$ hydrogel, PIWF$_1$, PIWF$_3$ and recycled hydrogels calculated from (d). Error bars represent the SD of the measured values (n = 3). (f) Strength comparison of PIWF$_3$ hydrogel (solid pentagram) and recycled IL/PVA hydrogel (hollow pentagram) with representative IL-based, organic/inorganic filler PVA hydrogels.

hydrogen bonds and crystal domains during the stretch-induced deformation process and their subsequent reorientations. After the first loading, the dissipated energy for 49 consecutive loading–unloading cycles tended to be stable. The recycled IL/PVA hydrogels exhibited remarkable fatigue resistance and decent electrical conductivity (Fig. S5 online).

In addition to excellent mechanical stability, BMIMBF$_4$/PVA hydrogels exhibited satisfactory thermal, electrical and radiation stability. The thermal decomposition temperature of the prepared PIWF$_3$ hydrogel was 317.92 °C, which was higher than 254.71 °C of PHF$_3$ hydrogel and 254.33 °C of PHF$_1$ hydrogel (Fig. S6a online). PIWF$_3$ hydrogels can also withstand continuous voltage output, maintaining a constant current in the voltage range of 0–2 V and a stable resistance at 2.0 V for 6 h (Fig. S6b, c online). After 0.5 h of exposure to UV light (λ = 253.7 nm), the properties of the PIWF$_3$ hydrogel remained unchanged, demonstrating its compatibility with the sterilization process for practical applications in wearable electronics (Fig. S6d online).

The impact of wet annealing on IL/PVA hydrogels was explored by assessing the relationship between viscosity and shear rate at two stages: prior to and following wet annealing. As shown in Fig. 2a, the gel before wet annealing exhibits obvious shear thinning behavior, indicating that its viscosity is relatively high, which makes it difficult to prepare a uniform sample in actual processing. On the contrary, after wet annealing, the gel transforms into a more fluid state (at room temperature), indicating that the heat treatment reduced the mutual entanglement between molecules. The importance of wet annealing for obtaining uniform IL/PVA hydrogels was also confirmed from the microstructural aspect. PHF_1 hydrogel has a porous structure (Fig. S7a online) due to the sparse PVA network and high-water content. After PVA and $BMIMBF_4$ were physically cross-linked but processed without wet annealing, the resulting hydrogel had uneven surface (Fig. S7b online). In contrast, $PIWF_3$ hydrogel treated with wet annealing displayed a more uniform structure and a highly interconnected compact network (Fig. S7c online). Meanwhile, wet annealing effectively improves tensile strength, toughness, and stretchability (PIF_3 and $PIWF_3$, Fig. S7d online). Therefore, based on the above results, the mechanical properties of IL/PVA hydrogels can be further optimized by adjusting the number of freeze–thaw cycles on the basis of wet annealing. This is because wet annealing enhances the hydration of the hydrogel and promotes the rearrangement of the internal cross-linked structure, while freeze–thaw cycles strengthen the cross-linked network, promote crystallization, and facilitate repair through repeated temperature changes, thereby increasing the mechanical strength and durability of the hydrogel [12]. In addition, wet annealing treatment was carried out on the sol formed from a high concentration of $BMIMBF_4$ solution (70 vol%) (Fig. S7e online). However, after 1 h of treatment at 90 °C, the sol partially became transparent, but the viscosity remained high, making it difficult to obtain a gel with uniform structure and properties.

The water contents of PHF_1, PIF_1, PIF_3, $PIWF_1$, and $PIWF_3$ hydrogels were 89.96%, 78.13%, 70.26%, 54.83%, and 49.91%, respectively (Fig. 2b online). The results showed that water was released in the cross-linking of PVA with $BMIMBF_4$, evaporated in wet annealing, and separated from the phase during freeze-thawing. The resulting $PIWF_3$ hydrogel had nearly 50% water content while demonstrating significantly enhanced mechanical properties. Fourier transform infrared spectroscopy (FT-IR) was used to analyze the internal molecular interactions of IL/PVA hydrogels (Fig. 2c online). The PVA peak at 3292 cm^{-1}, attributed to the –OH stretching vibration, exhibited a red shift and broadening after mixing with $BMIMBF_4$. This shift overlapped with the symmetric and asymmetric C–H stretching vibrations of the imidazolium cation ring (C4,5) at 3162 and 3120 cm^{-1}, indicating the formation of hydrogen bonds between PVA and $BMIMBF_4$ and the successful incorporation of the imidazolium cation. Additionally, the C4=C5 stretching

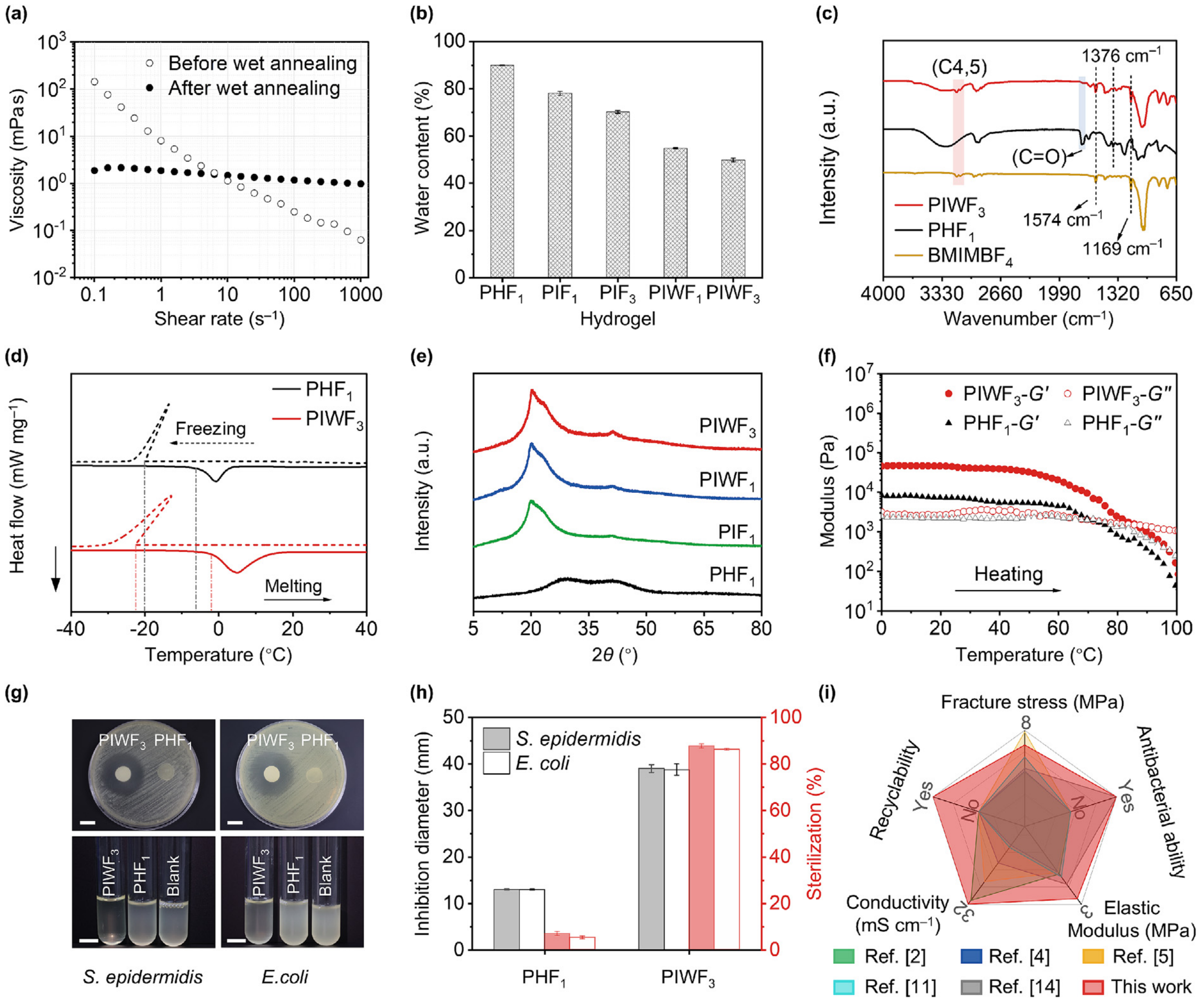

Fig. 2. Characterization of IL/PVA hydrogels. (a). Viscosity-shear rate curves for two intermediate states of IL/PVA hydrogels precursor (before and after wet annealing). (b) Water contents of PHF_1, PIF_1, $PIWF_1$ and $PIWF_3$ hydrogels. (c) FT-IR spectrum of $BMIMBF_4$, PHF_1 and $PIWF_3$ hydrogels. (d) DSC thermograph of PHF_1 and $PIWF_3$ hydrogels. (e) XRD patterns of PHF_1, PIF_1, $PIWF_1$ and $PIWF_3$ hydrogels. (f) Comparison of G' and G'' for PHF_1 and $PIWF_3$ hydrogels at different temperatures. (g) Photographs of PHF_1 and $PIWF_3$ hydrogels against *S. epidermidis* and *E. coli*. Scale bar: 1 cm. (h) The area of the inhibitory zone and the bactericidal ratio of PHF_1 and $PIWF_3$ hydrogels against *S. epidermidis* and *E. coli*. (i) Comparison of this work with recently reported PVA-based gel in terms of recyclability, conductivity, elastic modulus, antibacterial ability and fracture stress.

vibration of the imidazolium ring was observed at 1574 cm^{-1}, along with HCC and HCN bending modes at 1169 cm^{-1}. The C=O peak at 1730 cm^{-1} significantly weakened, which suggests the formation of strong hydrogen bonds, further confirming the successful integration of $BMIMBF_4$ into the hydrogel matrix and its strong interaction with PVA.

Differential scanning calorimetry (DSC) tests supported the above results (Fig. 2d). Compared to PHF_1 hydrogel, the freezing point of water in $PIWF_3$ hydrogel decreased significantly, while the melting point increased significantly. In the dense polymer network of $PIWF_3$ hydrogel, water freezes at approximately −22 °C and melts at around −1 °C. This temperature range is wider than that of PHF_1 hydrogel, where water in the sparse polymer network freezes at approximately −20 °C and melts at around −6 °C. X-ray diffraction (XRD) was conducted to examine the crystallinity of the PVA hydrogels (Fig. 2e). PHF_1 hydrogel has no obvious crystallization peak, while PIF_1, $PIWF_1$, and $PIWF_3$ hydrogels show distinct crystallization peaks and are significantly shifted relative to PHF_1 hydrogel. Specifically, the sharp peak centered at $2\theta = 20.12°$ corresponds to the (101) plane of the semicrystalline PVA, while the shoulder peak at 2θ = 23.34° and weak diffraction peak at 2θ = 41.33° were assigned to the (200) and (102) planes of the PVA, respectively. The results show that the physical cross-linking between IL and PVA greatly improves the crystallinity of PVA gel compared to simple freezing and thawing, and more freeze–thaw cycles further lead to an increase in the crystallinity of IL/PVA hydrogels. Fig. 2f shows the storage modulus (G') and loss modulus (G'') of the prepared PHF_1 hydrogel and $PIWF_3$ hydrogel as a function of temperature, reflecting the dynamic viscoelastic behavior of the hydrogels. G' and G'' of both hydrogels gradually decrease with increasing temperature and intersect around 72 and 86 °C, respectively. This intersection indicates that the corresponding $\tan\delta$ (G''/G', Fig. S8 online) of the two hydrogels equals 1 at these points, signifying the onset of the transformation from an elastic hydrogel to a viscoelastic liquid.

The introduction of IL not only enhanced the mechanical properties of the hydrogel, but also endowed it with excellent antibacterial ability, sensing capabilities (Figs. S9, S10 online) and the ability to construct all-in-one supercapacitors (Figs. S11, S12 online). Antibacterial ability is an important factor for the practical application of hydrogel materials in combination with biological tissues or on the skin for a long time. As shown in Fig. 2g, PHF_1 hydrogel produced solely by freeze-thawing lacks antibacterial properties, while $PIWF_3$ hydrogel showed excellent antibacterial activity. After 12 h of constant temperature culture, *Staphylococcus epidermidis* (ATCC6538, gram-positive organism) and *Escherichia coli* (ATCC25922, gram-negative organism) bacteria around $PIWF_3$ hydrogel were killed, and obvious inhibition rings appeared (Fig. 2g, upper part) with diameters of 38.33 and 37.92 mm, respectively (Fig. 2h). In addition, the turbidity of the PHF_1 hydrogel group solution was similar to that of the blank group, with almost no bactericidal effect. The solution in the $PIWF_3$ hydrogel group became almost clear and transparent (Fig. 2g, lower part), and had obvious bactericidal effects on both bacteria, with the bactericidal rates above 85% (Fig. 2h). Compared with representative PVA-based stretchable ionic electronics [2,4,5,11,14], IL/PVA hydrogels exhibit excellent conductivity, mechanical strength, recyclability and antibacterial ability (Fig. 2i). The excellent performance is due to the preferred materials and experimental methods. $BMIMBF_4$ serves a dual role: it functions as a cross-linker to enhance the hydrogel's flexibility and integrates into the polymer network as a conductive medium. The wet annealing process facilitates molecular rearrangement within the material, while the cyclic freeze–thaw process induces the formation of physical cross-links through crystalline PVA domains and hydrogen bonds, which act as energy dissipation zones. Consequently, the hydrogel exhibits a biphasic structure, balancing amorphous regions that facilitate ion transport with crystalline domains that provide mechanical strength. In addition, the imidazole groups on the ionic liquid have strong electrophilicity and hydrophilicity, which can interact with biomacromolecules (such as proteins and nucleic acids.) in bacterial cells, inhibiting the growth of bacteria or causing their death. The strain sensors prepared with $PIWF_3$ hydrogel and recycled IL/PVA hydrogel exhibit consistent linear sensitivity, short response and recovery times, excellent durability, and the ability to monitor finger movement (Figs. S9, S10 online). An all-in-one supercapacitor is obtained by in-situ formation of polyaniline (PANI) layers on both sides of the hydrogel. The introduction of PANI provides remarkable pseudocapacitance, and this integrated structure effectively reduces the electrolyte–electrode interface resistance, thereby maintaining excellent electrochemical performance even when stretched (Figs. S11, S12 online). The recycled IL/PVA hydrogel was processed into supercapacitors in the same manner as the original $PIWF_3$ hydrogel. Surprisingly, the recycled IL/PVA hydrogel-based supercapacitor exhibited highly consistent energy storage behaviors with the PANI/$PIWF_3$/PANI-based supercapacitor (Fig. S13a, b online), except that the capacitance was slightly lower than the latter at high current density (Fig. S13c online). A more detailed analysis of the strain sensors and supercapacitors can be found in the Supplementary materials (online).

In summary, this work developed highly tough and responsible hydrogels from IL and PVA. The obtained IL/PVA hydrogels have excellent strength of 4.99 MPa, high toughness of 2.52 MJ m^{-3}, elongation up to 1100%, and fatigue fracture resistance. These characteristics make the hydrogels suitable for use in various applications, such as strain sensors and supercapacitors, paving the way for the development of all-gel multi-modal flexible electronic devices. Furthermore, the prepared hydrogels demonstrate exceptional biocompatibility and can be easily recycled into new conductive materials through a simple heating process, underscoring their suitability for both human skins contact and environmentally sustainable practices. This work not only highlights the potential of these hydrogels for practical applications but also contributes to the advancement of green and flexible electronics.

Conflict of interest

The authors declare that they have no conflict of interest.

Acknowledgments

This work was supported by the National Natural Science Foundation of China (52303371), Guangdong Science and Technology Department (STKJ2023075, 2022A1515110209, and 2021B0301030005), Guangdong Education Department (2022KQNCX112), seed fund (GCII-Seed-202406) from GTIIT Changzhou Innovation Institute, and the Key Discipline (KD) Fund, the Technion, and the Start-Up Fund from Guangdong Technion.

Author contributions

Yan Wang conceived this concept and supervised the project. Pengcheng Zhou did the experiments and analyzed the data, and wrote the manuscript. Fan Mo gave help for the antibacterial test. Zichong Ji, Jiawei Yang, Hongzhong Du, and Zonglei Wang supported for the data analysis. Hossam Haick reviewed the manuscript and gave constructive suggestions. All authors discussed the results and commented on the manuscript.

Appendix A. Supplementary material

Supplementary data to this article can be found online at https://doi.org/10.1016/j.scib.2025.01.058.

References

[1] Lee S, Franklin S, Hassani FA, et al. Nanomesh pressure sensor for monitoring finger manipulation without sensory interference. Science 2020;370:966–70.

[2] Liu Y, Wang W, Gu K, et al. Poly(vinyl alcohol) hydrogels with integrated toughness, conductivity, and freezing tolerance based on ionic liquid/water binary solvent systems. ACS Appl Mater Interfaces 2021;13:29008–20.

[3] Yan CC, Li W, Liu Z, et al. Ionogels: preparation, properties and applications. Adv Funct Mater 2023;34:2314408.

[4] Li S, Li Y, Wang Y, et al. Highly stretchable, elastic, healable, and ultra-durable polyvinyl alcohol-based ionic conductors capable of safe disposal. CCS Chem 2022;4:3170–80.

[5] Ren Y, Guo J, Liu Z, et al. Ionic liquid-based click-ionogels. Sci Adv 2019;5:eaax0648.

[6] Mishra K, Devi N, Siwal SS, et al. Ionic liquid-based polymer nanocomposites for sensors, energy, biomedicine, and environmental applications: roadmap to the future. Adv Sci 2022;9:2202187.

[7] Sun B, Liu K, Wu B, et al. Low-hysteresis and tough ionogels via low-energy-dissipating cross-linking. Adv Mater 2024;36:2408826.

[8] Gong JY, Sun FC, Pan YC, et al. Stretchable and tough PAANa/PEDOT:PSS/PVA conductive hydrogels for flexible strain sensors. Mater Today Commun 2022;33:104324.

[9] Cheng Y, Zhu H, Li S, et al. Stretchable, low-hysteresis, and recyclable ionogel by ionic liquid catalyst and mixed ionic liquid-induced phase separation. ACS Sustainable Chem Eng 2023;11:15031–42.

[10] Huang Y, Wang Y, Guan X, et al. Unlimited recyclable wearable sensors based on a homogeneous ionic liquid and polyvinyl alcohol network. RSC Sustainability 2023;1:261–9.

[11] Zhang Z, Sang M, Pan Y, et al. Ionic liquid-reinforced transparent, stretchable, conductive organic ionic gel with ultra-high sensory capability and ultra-robust impact-resistance. Chem Eng J 2024;496:154227.

[12] Wu Y, Zhang Y, Wu H, et al. Solvent-exchange-assisted wet annealing: a new strategy for superstrong, tough, stretchable, and anti-fatigue hydrogels. Adv Mater 2023;35:e2210624.

[13] Kamio E, Yasui T, Iida Y, et al. Inorganic/organic double-network gels containing ionic liquids. Adv Mater 2017;29:1704118.

[14] Xu Q, Hou M, Wang L, et al. Anti-bacterial, anti-freezing starch/ionic liquid/PVA ion-conductive hydrogel with high performance for multi-stimulation sensitive responsive sensors. Chem Eng J 2023;477:147065.

[15] Zhou Y, Zhang L, Lin X, et al. Dual-network polyvinyl alcohol/polyacrylamide/xanthan gum ionic conductive hydrogels for flexible electronic devices. Int J Biol Macromol 2023;233:123573.

[16] Hua M, Wu S, Ma Y, et al. Strong tough hydrogels via the synergy of freeze-casting and salting out. Nature 2021;590:594–9.

[17] Hao M, Wang Y, Li L, et al. Tough engineering hydrogels based on swelling–freeze–thaw method for artificial cartilage. ACS Appl Mater Interfaces 2022;14:25093–103.